

REPORT DOCUMENTATION PAGE			Form Approved OMB NO. 0704-0188		
<p>The public reporting burden for this collection of information is estimated to average 1 hour per response, including the time for reviewing instructions, searching existing data sources, gathering and maintaining the data needed, and completing and reviewing the collection of information. Send comments regarding this burden estimate or any other aspect of this collection of information, including suggestions for reducing this burden, to Washington Headquarters Services, Directorate for Information Operations and Reports, 1215 Jefferson Davis Highway, Suite 1204, Arlington VA, 22202-4302. Respondents should be aware that notwithstanding any other provision of law, no person shall be subject to any penalty for failing to comply with a collection of information if it does not display a currently valid OMB control number.</p> <p>PLEASE DO NOT RETURN YOUR FORM TO THE ABOVE ADDRESS.</p>					
1. REPORT DATE (DD-MM-YYYY)		2. REPORT TYPE		3. DATES COVERED (From - To)	
		New Reprint		-	
4. TITLE AND SUBTITLE Enhanced Bioactivity of Internally Functionalized Cationic Dendrimers with PEG Cores			5a. CONTRACT NUMBER		
			5b. GRANT NUMBER W911NF-09-D-0001		
			5c. PROGRAM ELEMENT NUMBER 611104		
6. AUTHORS L. Albertazzi, F. M. Mickler, G. M. Pavan, F. Salomone, G. Bardi, M. Panniello, E. Amir, T. Kang, K. L. Killops, C. Bräuchle, R. J. Amir, C. J. Hawke			5d. PROJECT NUMBER		
			5e. TASK NUMBER		
			5f. WORK UNIT NUMBER		
7. PERFORMING ORGANIZATION NAMES AND ADDRESSES University of California - Santa Barbara 3227 Cheadle Hall 3rd floor, MC 2050 Santa Barbara, CA 93106 -2050			8. PERFORMING ORGANIZATION REPORT NUMBER		
9. SPONSORING/MONITORING AGENCY NAME(S) AND ADDRESS(ES) U.S. Army Research Office P.O. Box 12211 Research Triangle Park, NC 27709-2211			10. SPONSOR/MONITOR'S ACRONYM(S) ARO		
			11. SPONSOR/MONITOR'S REPORT NUMBER(S) 55012-LS-ICB.570		
12. DISTRIBUTION AVAILABILITY STATEMENT Approved for public release; distribution is unlimited.					
13. SUPPLEMENTARY NOTES The views, opinions and/or findings contained in this report are those of the author(s) and should not be construed as an official Department of the Army position, policy or decision, unless so designated by other documentation.					
14. ABSTRACT See attached.					
15. SUBJECT TERMS See attached.					
16. SECURITY CLASSIFICATION OF:		17. LIMITATION OF ABSTRACT	15. NUMBER OF PAGES	19a. NAME OF RESPONSIBLE PERSON	
a. REPORT	b. ABSTRACT			c. THIS PAGE	Francis Doyle
UU	UU	UU		19b. TELEPHONE NUMBER	
				805-893-8133	

Report Title

Enhanced Bioactivity of Internally Functionalized Cationic Dendrimers with PEG Cores

ABSTRACT

See attached.

REPORT DOCUMENTATION PAGE (SF298)
(Continuation Sheet)

Continuation for Block 13

ARO Report Number 55012.570-LS-ICB
Enhanced Bioactivity of Internally Functionalized ...

Block 13: Supplementary Note

© 2012 . Published in Biomacromolecules, Vol. Ed. 0 13, (0) (2012), (, (0). DoD Components reserve a royalty-free, nonexclusive and irrevocable right to reproduce, publish, or otherwise use the work for Federal purposes, and to authorize others to do so (DODGARS §32.36). The views, opinions and/or findings contained in this report are those of the author(s) and should not be construed as an official Department of the Army position, policy or decision, unless so designated by other documentation.

Approved for public release; distribution is unlimited.

Enhanced Bioactivity of Internally Functionalized Cationic Dendrimers with PEG Cores

Lorenzo Albertazzi,^{†,‡,§} Frauke M. Mickler,[§] Giovanni M. Pavan,^{||} Fabrizio Salomone,^{‡,§} Giuseppe Bardi,[§] Mariangela Panniello,^{‡,§} Elizabeth Amir,[†] Taegon Kang,[†] Kato L. Killops,[⊥] Christoph Bräuchle,[§] Roey J. Amir,^{*,†,‡,§} and Craig J. Hawker^{*,†}

[†]Materials Research Laboratory, University of California, Santa Barbara, California 93106-5121, United States

[‡]NEST, Scuola Normale Superiore and Istituto Nanoscienze-CNR, Piazza San Silvestro 12-56127 Pisa, Italy

[§]Center for Nanotechnology Innovation @NEST, Istituto Italiano di tecnologia, Piazza San Silvestro 12, 56127 Pisa, Italy

[§]Department of Chemistry, Ludwig-Maximilians-Universität München, Center for NanoScience (CeNS) and Center for Integrated Protein Science Munich (CIPSM), Butenandtstr. 5-13, D-81377 München, Germany

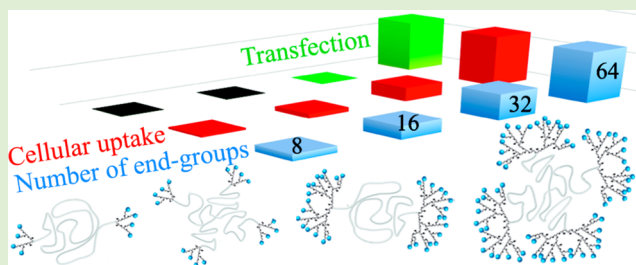
^{||}Laboratory of Applied Mathematics and Physics (LaMFI), University of Applied Sciences of Southern Switzerland (SUPSI), Centro Galleria 2, Manno, 6928, Switzerland

[⊥]U.S. Army RDECOM Edgewood Chemical Biological Center, Aberdeen Proving Ground, Maryland 21010, United States

[#]Department of Organic Chemistry, School of Chemistry, Faculty of Exact Sciences, Tel-Aviv University, Tel-Aviv 69978, Israel

S Supporting Information

ABSTRACT: Hybrid dendritic-linear block copolymers based on a 4-arm poly(ethylene glycol) (PEG) core were synthesized using an accelerated AB₂/CD₂ dendritic growth approach through orthogonal amine/epoxy and thiol-yne chemistries. The biological activity of these 4-arm and the corresponding 2-arm hybrid dendrimers revealed an enhanced, dendritic effect with an exponential increase in cell internalization concomitant with increasing amine end groups and low cytotoxicity. Furthermore, the ability of these hybrid dendrimers to induce endosomal escape combined with their facile and efficient synthesis makes them attractive platforms for gene transfection. The 4-arm-based dendrimer showed significantly improved DNA binding and gene transfection capabilities in comparison with the 2-arm derivative. These results combined with the MD simulation indicate a significant effect of both the topology of the PEG core and the multivalency of these hybrid macromolecules on their DNA binding and delivery capabilities.



INTRODUCTION

The modular structure, plurality of functional end groups, and monodispersity of dendrimers make them appealing scaffolds for biomedicine,^{1–7} enabling a broad spectrum of applications including visualization of subcellular processes⁸ as delivery agents^{9,10} and as scaffolds for vaccines/antiviral agents.^{11–13} While well-suited for these architectures, the synthesis of dendrimers is still considered to be a time-consuming process requiring rigorous purification processes.¹⁴ Furthermore, partial functionalization with bioactive moieties, which are often hydrophobic, leads to low loading and results in polydisperse materials.¹⁵

To address these challenges and simplify their preparation, several groups have reported the use of polyethylene glycol (PEG) as a difunctional or monofunctional polymeric core for the divergent synthesis of dendrimers.^{16–18} These strategies rely on the solubility of the PEG core to simplify purification of the PEG-dendrimer hybrids by dialysis or precipitation. Additionally, Park and coworkers demonstrated increased

colloidal stability and reduced toxicity for PAMAM-PEG-PAMAM copolymers when compared with commercial PAMAM dendrimers.¹⁹ Recently, we reported the accelerated synthesis of internally functionalized PEG-dendrimer hybrids and their application as a dual-functional delivery platform.²⁰ On the basis of a bifunctional PEG core, a fourth-generation dendrimer with 32 orthogonal surface groups and 20 internal functionalities was synthesized in only four steps. The success of this approach prompted the exploration of alternative hybrid dendritic architectures to understand their structure–property relationship with respect to biological activity.

Herein we report the synthesis of amine-terminated hybrid dendrimers, based on a 4-arm PEG star core, in only four steps, with precipitation and dialysis as the only means of purification. The facile synthesis, simple purification, and compatibility of

Received: September 3, 2012

Revised: November 4, 2012

Published: November 9, 2012

the alkyne groups of the third generation with both thiol-ene^{21–23} and copper-catalyzed azide–alkyne^{24–26} click chemistries make these dendrimers highly attractive scaffolds for various biomedical applications. The role of architecture and number of end groups in determining the interaction of these 2-arm and 4-arm based hybrid cationic dendrimers with living cells was evaluated with respect to toxicity, membrane affinity, and internalization pathway (Figure 1).

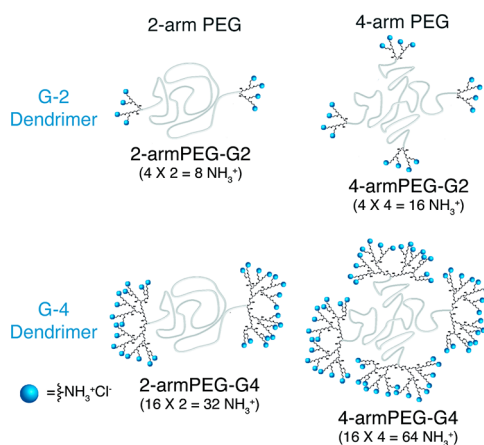


Figure 1. Schematic representation of the structures of second and fourth generations of 2-armPEG-G_n and 4-armPEG-G_n series with increasing number of cationic amines at the chain ends.

EXPERIMENTAL SECTION

Materials. All solvents (ACS grade, Fisher) were used as received. Tetra-amine PEG 10K was purchased from Laysan Bio. 2,2'-Azobis(2-methylpropionitrile) (98%), cysteamine hydrochloride (98%) and 2,2-dimethoxy-2-phenylacetophenone (99%) were purchased from Aldrich. Glycidyl propargyl ether (GPE, technical >90%, Santa Cruz Biotechnology), *N,N*-diisopropylethylamine (98%, TCI America), Alexa Fluor 488 and 647 (Invitrogen), and deuterated solvents for NMR (Cambridge Isotope Laboratories, Inc.) were used as received. Dialysis tubes (regenerated cellulose, spectra/por 6, MWCO 1K) were purchased from Spectrum Laboratories. Dendrimers 2-armPEG-G2 and 2-armPEG-G4 were synthesized as previously reported.²⁰

Instrumentation. ¹H and ¹³C NMR spectra were recorded on Varian 500 or Bruker Avance III 800 spectrometers, respectively. Chemical shifts are reported in ppm and referenced to the solvent signal. The molecular weights of the dendrimers were determined by comparison of the areas of the peaks corresponding to the PEG block (3.63 ppm) and the proton peaks of the dendrimers. Infrared spectra were recorded on a Perkin-Elmer Spectrum 100 with a Universal ATR sampling accessory. Gel permeation chromatography (GPC) analysis was performed on a Waters Alliance instrument equipped with three columns: Eprogen, CATSEC 100, 300, and 1000 Å with 1 wt % acetic acid/0.10 M sodium sulfate (aq) as eluent (flow rate: 0.25 mL/min at 25 °C). Detection was achieved with Waters photodiode array (PDA) and refractive index (RI) detectors with linear PEG standards used for calibration. MALDI-TOF samples were run on a Voyager DE Pro (Applied Biosystems Instruments) using a stainless-steel sample plate. All matrices (2,5-dihydroxybenzoic acid, α -cyano-4-hydroxycinnamic acid, dithranol, and sinapinic acid) were purchased from Sigma Aldrich and used without further purification. Dynamic light scattering (DLS) was conducted with a Wyatt DynaPro NanoStar equipped with a 100 mW, 662 nm air-launched laser and a detector at a constant angle of 90°. Solutions of dendrimers 2-armPEG-G4 and 4-armPEG-G4 were prepared using PBS buffer pH 7.4 (buffer was filtered using a Nylon 0.45 μ m filter prior to sample preparation). Samples were mixed using a vortex shaker for 1 min and then filtered through Nylon 0.45 μ m filters. Measurements were carried at 25 °C using disposable cuvettes.

Synthesis of Dendrimers. **Dendrimer 4-armPEG-G1.** 10kD tetra-amine PEG (1.00 g, 0.1 mmol) was dissolved in MeOH (5.0 mL), GPE (1.70 mL, 16.0 mmol) was added, and the reaction was stirred overnight. The crude mixture was precipitated into ether, and the product was collected by filtration and dried overnight in a vacuum oven at 40 °C to give the tetraalkyne dendrimer 4-armPEG-G1 (960 mg, 88% yield) in the form of white powder. FT-IR, ν (cm⁻¹): 3240, 2880, 1460, 1360, 1340, 1280, 1240, 1150, 1100, 1060, 960, 840. ¹H NMR (500 MHz, CDCl₃) δ : 4.19–4.14 (m, O–CH₂–alkyne), 3.86–3.45 (CH–O and CH₂–O of dendrimer; CH₂ of PEG backbone), 3.38 (s, C–(CH₂–O)₄ of the PEG core), 2.89–2.42 (m, CH₂N and alkyne-H). ¹³C NMR (200 MHz, CDCl₃) δ : 79.7, 74.7, 71.7, 70.4, 68.4, 67.3, 59.3, 58.3, 58.2, 55.4, 54.4.

Dendrimer 4-armPEG-G2. Dendrimer 4-armPEG-G1 (500 mg, 0.046 mmol), cysteamine hydrochloride (1.7 g, 15 mmol), and DMPA (38 mg, 0.15 mmol) were dissolved in MeOH (5 mL). The mixture was purged with argon for 10 min and then irradiated under UV irradiation for 1 h. MeOH (5 mL) was subsequently added, and the crude mixture dialyzed against DI water (3 \times 1.0 L) for 24 h. The solution was then removed from the dialysis tube, and the solvent was removed by freeze-drying to give the dendrimer 4-armPEG-G2 (464 mg, 80% yield) in the form of white solid. FT-IR, ν (cm⁻¹): 3410, 2880, 1470, 1360, 1340, 1280, 1240, 1150, 1100, 1060, 960, 840. ¹H NMR (500 MHz, DMSO-*d*₆) δ : 8.15 (br, NH₃⁺), 3.74–3.39 (m, CH–O and CH₂–O of dendrimer; CH₂ of PEG backbone; CH₂NH₃⁺ and C–(CH₂–O)₄ of the PEG core), 3.19–2.78 (m, CH₂N; CHS and CH₂S). ¹³C NMR (200 MHz, DMSO-*d*₆) δ : 72.7, 72.1, 70.7, 69.6, 68.9, 44.4, 38.6, 33.3, 28.7, 27.4.

Dendrimer 4-armPEG-G3. Dendrimer 4-armPEG-G2, (460 mg, 0.036 mmol) was dissolved in MeOH (3.0 mL), GPE (5 mL, 46 mmol) and DIPEA (0.2 mL, 1.2 mmol) were added, and the reaction was stirred overnight at room temperature. The crude mixture was precipitated into ether, and the product was collected by filtration and dried overnight in a vacuum oven at 40 °C to give dendrimer 4-armPEG-G3 (549 mg, quantitative) in the form of very light-yellow powder. FT-IR, ν (cm⁻¹): 3240, 2920, 2850, 1460, 1350, 1300, 1250, 1090, 950, 850. ¹H NMR (500 MHz, CDCl₃) δ : 4.19 (m, O–CH₂–alkyne), 3.89–3.35 (m, CH–O and CH₂–O of dendrimer; CH₂ of PEG backbone and C–(CH₂–O)₄ of the PEG core), 3.10–2.41 (m, CHS; CH₂S; CH₂N and alkyne-H). ¹³C NMR (200 MHz, CDCl₃) δ : 79.7, 78.5, 77.9, 75.0, 73.6, 73.2, 71.8, 70.5, 70.3, 68.3, 58.6, 58.4, 55.0, 54.7, 45.8, 35.0, 31.5, 30.1.

Dendrimer 4-armPEG-G4. Dendrimer 4-armPEG-G3 (100 mg, 6.4 μ mol), cysteamine hydrochloride (930 mg, 8.2 mmol), and DMPA (21 mg, 0.082 mmol) were dissolved in MeOH (2.0 mL). The mixture was purged with argon for 15 min and then irradiated under UV irradiation for 1 h. The solvent was evaporated, and the crude mixture was dissolved in DI water (10.0 mL) and dialyzed against DI water (3 \times 1.0 L) for 24 h, followed by lyophilization to yield amino-functionalized dendrimer 4-armPEG-G4 in the form of yellow solid (129 mg, 88% yield). FT-IR, ν (cm⁻¹): 3380, 2880, 1610, 1470, 1340, 1280, 1240, 1100, 950, 840. ¹H NMR (500 MHz, DMSO-*d*₆) δ : 8.24 (br, NH₃⁺), 3.80–3.21 (m, CH–O and CH₂–O of dendrimer; CH₂ of PEG backbone; CH₂NH₃⁺ and C–(CH₂–O)₄ of the PEG core), 3.19–2.56 (m, CH₂N; CHS and CH₂S). ¹³C NMR (200 MHz, DMSO-*d*₆) δ : 73.3, 72.0, 70.2, 69.6, 69.1, 67.4, 44.8, 38.7, 33.4, 28.5, 27.5.

General Procedure for Fluorophore Labeling of Dendrimers.

Dendrimers were conjugated with Alexa488 or Alexa647 fluorophores to afford labeled dendrimers following previously reported procedure.^{27,28} In brief, conjugation was carried out via amide bond formation between the primary amine of the dendrimer and the *N*-hydroxysuccinimide activated carboxyl of the fluorophores. Dendrimers (50 nmol) were dissolved in DMSO, the reactive dye (1 equiv) was added, and the solution was stirred for 4 h at room temperature and then dialyzed against water (MWCO = 10 kDa) to afford the desired dendrimer–dye conjugates, with an estimated average of one dye per dendrimer. The fluorescence intensity of different dendrimers was evaluated and normalized to account for differences in their brightness.

Table 1. Experimental and Theoretical Molecular Weights of Dendrimers 4-armPEG-Gn

	M_n (GPC) ^a	PDI	M_p (MALDI) ^b	theoretical M_n
4-armPEG-G0	12 000	1.21	10 700	10 000
4-armPEG-G1	NA ^a	NA ^a	11 300	10 900
4-armPEG-G2	17 600	1.25	12 100	12 700
4-armPEG-G3	NA ^a	NA ^a	13 200	15 700
4-armPEG-G4	23 800	1.19	ND ^c	23 000

^aAqueous phase cationic GPC was used to determine M_n and PDI of the positively charged dendrimers. Data for the alkyne-terminated dendrimers are not available (NA) because they were not analyzed due to their poor solubility and aggregation in the mobile phase. ^b M_p : maximum of molecular ion peaks. ^cND: not detectable.

Flow Cytometry Measurements. HeLa cells were grown in a six-well plate and after treatment with Alexa488-labeled dendrimer were detached using trypsin-EDTA, washed with PBS buffer, and fixed with 4% paraformaldehyde (PFA). Cells were washed with PBS until complete removal of PFA and finally resuspended in 250 μ L of PBS. Flow cytometry was performed on a MACSQuant system (Miltenyi) by counting 10 000 events.

Cell Culture and Confocal Imaging. HeLa (CCL-2) were purchased from ATCC and cultured following manufacturer's instructions. For live cell, microscopy cells were plated onto 35 mm glass-bottomed dishes (WillCo-dish GWSt-3522) and imaged at 37 °C 5% CO₂.

Cell imaging was performed on a Leica TCS SP2 inverted confocal microscope (Leica Microsystems) equipped with a 40 \times 1.25 NA oil immersion objective (Leica Microsystems). Imaging was obtained illuminating the samples with the inline Ar and He-Ne lasers of the microscope and with a 403 nm pulsed diode laser (M8903-01;

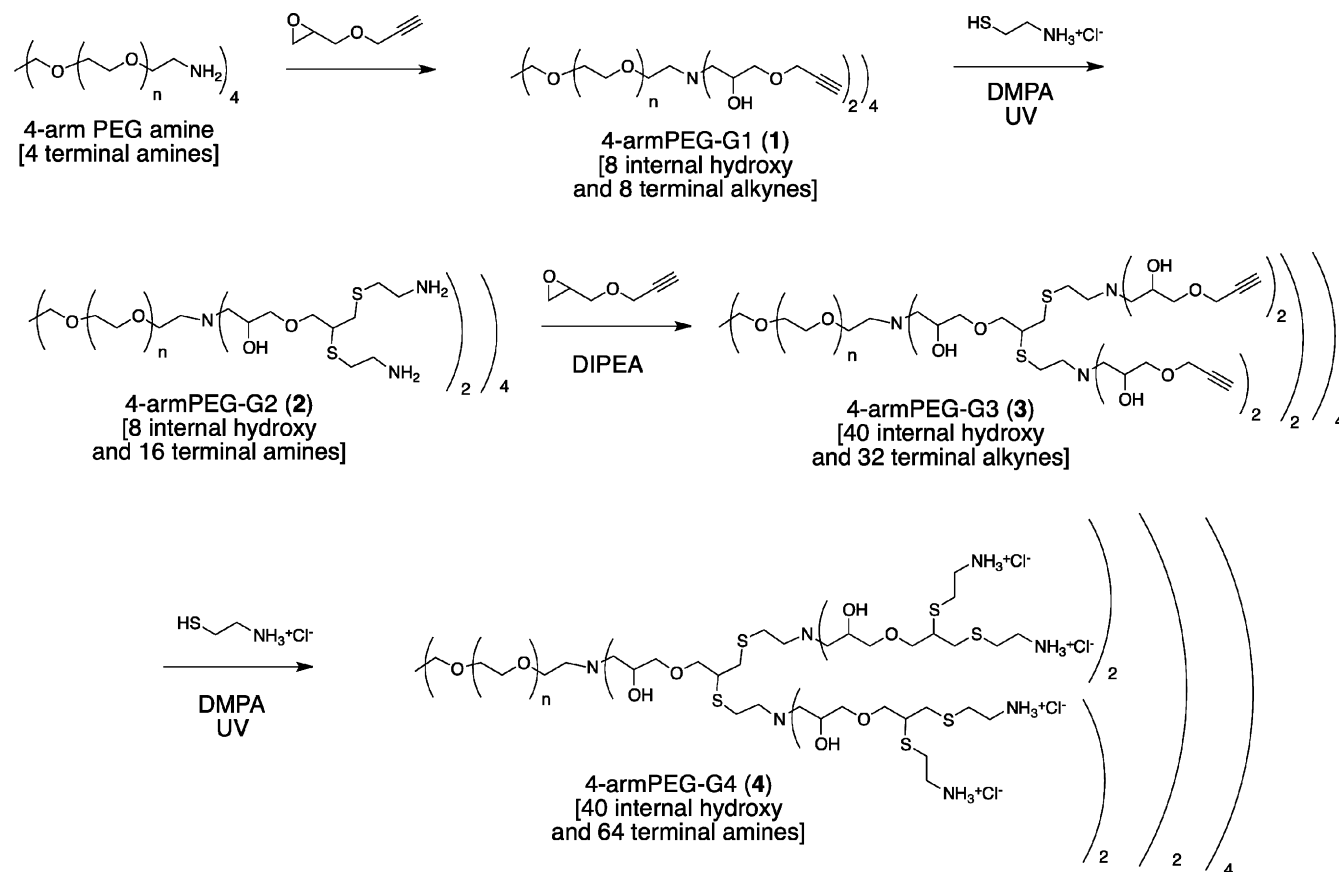
Hamamatsu) at 50 MHz repetition rate. Fluorescence emission was collected with the AOBs-based built-in detectors of the confocal microscope (Hamamatsu R6357).

For the toxicity assay, HeLa cells were incubated for 2 h at 37 °C with DMEM containing 8 μ g/mL propidium iodide (PI), 1 μ g/mL of calcein AM, and different concentrations of dendrimers. The medium was then discarded and the cells were washed with PBS buffer containing the same concentration of PI before confocal imaging.

Internalization Assay and Colocalization Studies. To monitor dendrimer internalization, cells were incubated with 100 nM labeled dendrimers in DMEM for 1 h at 37 °C. To remove unbound molecules from the medium, we rinsed cells two times with PBS. After the initial preloading and subsequent washing, cells were incubated again in DMEM and imaged at the indicated time point. To identify the endocytic vesicles involved in dendrimer internalization, we performed colocalization assays in living cells. For this, HeLa cells were coinoculated with dendrimers (as described above) and different dyes: these include 1 mg/mL 70 kDa dextran-FITC conjugate at 37 °C for 30 min to label macropinosomes, 50 mM LysoSensor for 10 min to label lysosomes, and 2 μ g/mL transferrin Alexa488 conjugate to label recycling and sorting endosomes. Images were analyzed using ImageJ software version 1.37 (NIH Image; <http://rsbweb.nih.gov/ij/>).

Endosomal Escape Assay. For a typical calcein assay, cells were seeded 24 h before the experiment in WillCo-dishes to reach a 70% confluence. Medium was replaced with 1.0 mL of DMEM containing the dendrimer together with 250 μ M of calcein. After 2 h of incubation at 37 °C, cells were washed three times with PBS and then analyzed by confocal microscopy.

Ethidium Bromide Intercalation Assay. Ethidium bromide (EB, 1 μ g/mL) and DNA (3 μ g/mL) were dissolved in 0.05 mol/L Tris-HCl buffer with 50 mmol/L NaCl (pH 7.4). The fluorescence spectra of EB in the presence of DNA before and after the addition of dendrimers were taken with a Cary Eclipse fluorimeter. EB was excited

Scheme 1. Synthesis of 4-armPEG-G4 Dendrimer, 4, with 40 Internal OH Groups and 64 Terminal NH₂ Groups

at 477 nm, and the emission spectra were recorded from 490 to 850 nm. A sample of EB with dendrimer was studied to check that no interaction of the macromolecule with the dye is present.

Transfection Experiments and Confocal Imaging. HeLa cells were grown in DMEM (Invitrogen) supplemented in 10% FCS at 37 °C and 5% CO₂. For imaging experiments, cells were seeded in eight-well chambered ibiTreat μ -Slides (Ibidi, Munich, Germany) at a density of 10000 cells per well. Plasmid DNA (pCMVLuc) was labeled with Cy5 fluorophore using the Label IT kit (MIRUS, Madison, WI) according to the manufacturer's instructions. Dendriplexes were generated by incubating DNA (Cy5-labeled pCMVLuc for single-particle imaging experiments, unlabeled pEGFPNuc for gene expression) with different dendrimers at N/P = 4 for 30 min at room temperature in HBG buffer (20 mM Hepes pH 7.1, 5% glucose w/v). Twenty μ L of dendriplexes equivalent to 400 ng DNA was administered to cells in a total volume of 240 μ L serum-free CO₂ independent cell medium (Invitrogen). Cells were washed three times in PBS buffer (either after 1h or 5h) and incubated in CO₂ independent medium supplemented with 10% FCS. Single cells were analyzed on a heated microscope stage by spinning disk confocal microscopy using a Nikon TE2000E microscope, the Yokogawa CSU10 spinning disk unit, an EM-CCD camera (iXon DV884; Andor), and a Nikon 1.49 NA 100 \times Plan Apo oil immersion objective. Cells were imaged after either 1 or 22 h. Z-stacks were imaged with 641 nm laser excitation at 300 ms per frame and with a spacing of 166 nm between two planes. Z-projections of the recorded image sequences were built in Image J. GFPNuc expression was detected by widefield microscopy on a custom build setup based on a Nikon Ti microscope equipped with a 10 \times or 20 \times objective. The total fluorescence signal per field of view was calculated in ImageJ by summing all pixel intensities above a set intensity threshold. To analyze the fluorescence intensity per dendriplex, we identified single particles in ImageJ using a defined size restriction and an intensity threshold criterion.

RESULTS AND DISCUSSION

Synthesis. 4-armPEG-Gn dendrimers of generations 1–4 were synthesized using a sequence of amine/epoxy and thiol/yne reactions as presented in Scheme 1. The 10 kDa 4-arm PEG amine, which serves as a core, and an excess of commercially available GPE were stirred in methanol overnight to give the hybrid dendrimer 4-armPEG-G1 (1) in 88% yield after precipitation in ether. Subsequent thiol-yne reaction with excess cysteamine hydrochloride gave 4-armPEG-G2 (2) in 80% yield after dialysis. Repetition of this two-step epoxy ring-opening/thiol-yne growth strategy then gave 4-armPEG-G3 (3) in near quantitative yields with the fourth-generation hybrid dendrimer 4-armPEG-G4 (4) being obtained in 88% after sequential thiol-yne reaction, followed by dialysis.

This accelerated dendritic growth strategy, coupled to a starting tetravalent PEG-core, allows a fourth-generation dendrimer, having a total of 64 chain end amino groups and 40 internal hydroxy functional groups, to be prepared in only four steps. Furthermore, the high-molecular-weight 4-arm PEG core (10 kDa) permits the use of precipitation or dialysis as the only means of purification, greatly simplifying the synthetic process.

Dendrimer–Cell Interactions. Previous studies have shown that overall structure, generation, and number of functional groups have important implications for biological activity of various dendrimers.^{27–36} Thus, an extensive evaluation of the interactions of 2-arm and 4-arm PEG-dendrimer hybrids with living cells was carried out with particular attention to toxicity, cell internalization ability, and their capability to induce endosomal escape, which are three crucial factors relevant for intracellular delivery applications. To

study the biological properties of these dendrimers by confocal microscopy and flow cytometry (FACS), we fluorescently labeled the PEG-dendrimer hybrids with Alexa-488.

Toxicity Assay. Cell viability with respect to dendrimer structure and concentration was assessed by a PI and calcein acetoxymethyl ester (AM) assay. PI dye cannot permeate intact cell membranes, and it can be internalized only when the membrane is defective, which allows monitoring of cell viability as PI permeates only dead cells. The calcein AM dye readily passes through the cellular plasma membrane into the cytoplasm, where the acetyl groups are cleaved by esterases to yield the more hydrophilic calcein. Trapped inside the cell, the calcein can readily bind to intracellular calcium, resulting in a strong fluorescence. Because dead cells lack cytoplasmic esterases, fluorescence is observed only in live cells. Figure 2

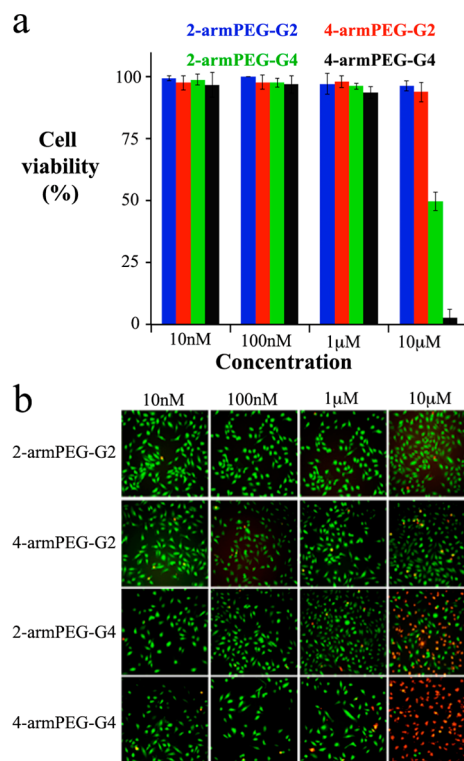


Figure 2. Dendrimer toxicity in HeLa cells. The histogram (a) reports the cell viability measured with PI/calcein AM assay after cells incubation with different amount of dendrimer. (b) Imaging of calcein AM (green = live cells) and PI (red = dead cells).

shows images of PI (in red) and calcein AM (in green) in HeLa cells incubated with dendrimers at 10 nM, 100 nM, 1.0 μ M, and 10 μ M concentrations. High cell viability was observed for all dendrimers up to a concentration of 1.0 μ M, and the compounds were found to be toxic only at a concentration of 10 μ M. At this concentration, the dendrimers' toxicity is correlated to the number of functional groups, as the higher generation dendrimers show higher toxicity, which agrees well with previous reports of cationic PAMAM dendrimers containing an equivalent number of end groups.²⁷

Cellular Uptake. A flow cytometry assay was performed to quantify cell uptake of different dendrimers. On the basis of the toxicity results, we expected the hybrid dendrimers to show a similar trend in their membrane affinity, and consequently in cell internalization, when compared with cationic dendrimers where higher cells affinities typically correlate with higher cell

toxicity. HeLa cells were incubated for 30 min with the dendrimers, and the membrane binding was quantified by flow cytometry. The FACS (Figure 3) results indicate negligible

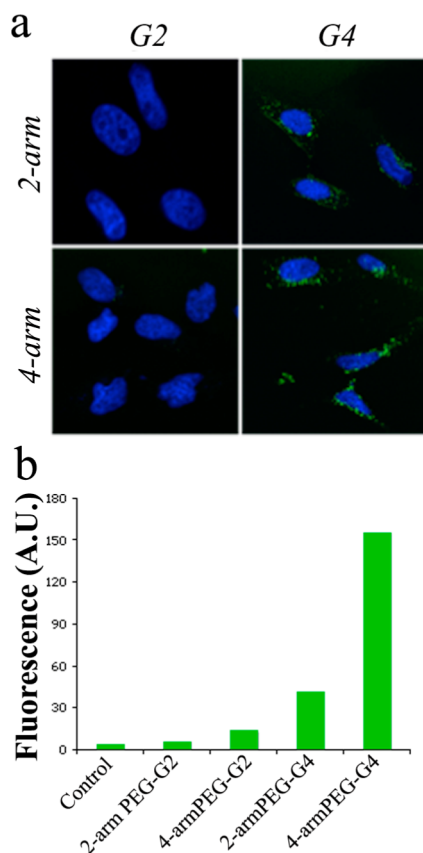


Figure 3. Cell binding and internalization. (a) Confocal imaging of HeLa cells treated with AF488-labeled dendrimers at 100 nM concentration (nuclei were visualized with Hoechst (blue)) and (b) membrane binding quantification of HeLa cells treated for 30 min with PEG-dendrimer hybrids.

binding for the smaller second-generation 2-armPEG and 4-armPEG dendrimers. In direct contrast, membrane affinity was observed to increase as the number of end groups increased with a notable exponential jump for the fourth-generation 4-arm derivative. This nonlinear trend cannot be explained by a simple, increased number of charged ammonium moieties at the chain ends of the dendrimers, and the pronounced difference in performance between the 2-arm and 4-arm hybrid dendrimers must be due to the influence of the core architecture. To further understand the origin of this promising balance between toxicity and cell affinity for the fourth-generation, 4-arm derivative, we undertook an in-depth analysis of the solution structure and their biological performance as a gene delivery platform.

Internalization Pathways. To identify the biological pathways involved in internalization of these hybrid dendritic macromolecules, we performed colocalization assays with biomarkers for different endocytic vesicles. Transferrin-Alexa 488 and 70 kDa dextran-FITC were used to trace clathrin-dependent endocytosis and macropinocytosis, respectively. Preliminary studies showed the colocalization of the 4-arm, fourth-generation PEG-dendrimer, 4, with the dextran marker (Figure 4), which suggests internalization by macropinocytosis with the clathrin-mediated pathway not playing a significant

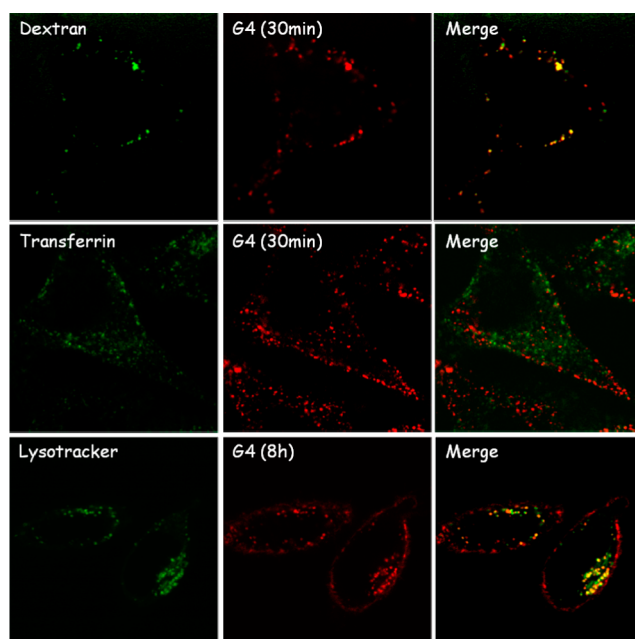


Figure 4. Colocalization of 4-armPEG-G4 dendrimer (100 nM, in red) with endocytic vesicle markers (in green). Strong colocalization signal was observed for the macropinocytosis marker (top) and lysosome marker (bottom).

role. Interestingly these results differ from what is observed for PAMAM dendrimers that are internalized both via micropinocytosis and clathrin-mediated endocytosis²⁷ but are in good agreement with recently reported studies of other PEG-dendrion hybrids.^{28,37} More detailed studies showed that the dendrimers reach their final destination in the perinuclear region in ca. 8h, and a colocalization assay with lysotracker at this time point showed localization in the lysosomal compartment, similarly to other cationic dendrimers such as PAMAM.²⁷ No further changes in localization have been observed after lysosomal delivery up to 48 h, suggesting the lysosome represents the final destination of dendrimers inside the cell. This lysosomal localization is of particular interest for delivery applications owing to the low pH and high activity of hydrolytic enzymes in this compartment, which allows for the design of tailored dendritic platforms responsive to the specific biochemical properties of the lysosome.^{20,37}

Endosomal Escape. In a recent report, we showed the release of coumarin dyes from a 2-armPEG-G4 in B16 cells.²⁰ After cleavage of covalently loaded coumarins from the dendritic carrier, the released dyes showed a cytoplasmic localization, while the dendrimers remained in the endolysosomal system. To investigate the role of our hybrid dendrimers on the endosomal escape of covalently attached dye molecules, we investigated the ability of the dendrimers to induce endosomal escape of coinubated calcein. Figure 5 shows confocal fluorescence images of HeLa cells after treatment with calcein alone or with a mixture of calcein and the 2- and 4-arm fourth-generation dendrimers. As can be seen in the upper panel, cells incubated only with calcein show green fluorescence localized in endocytic vesicles, with no signal coming from the cytoplasm. This is expected because the hydrophilicity of the calcein molecules does not allow them to penetrate the membrane of the vesicles, and hence the molecules are locked within endosomal and lysosomal vesicles. In direct contrast, for cells incubated with the 2- and 4-arm fourth-generation

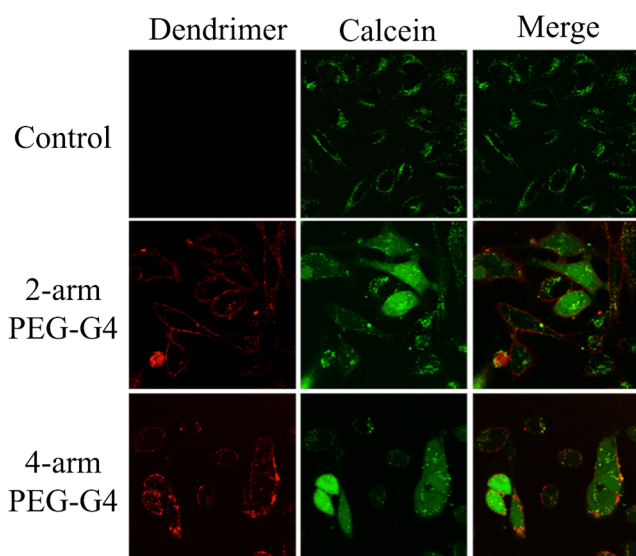


Figure 5. HeLa cells treated with calcein only (top), calcein with 200 nM 2-armPEG-G4 dendrimer (middle), and calcein with 200 nM 4-armPEG-G4 dendrimer (bottom). Calcein and dendrimer fluorescence is represented in green and red, respectively.

dendrimers, green fluorescence from calcein is observed in the cytoplasm, demonstrating that the dendrimers are able to destabilize vesicles and allow for the escape of small molecules. Notably the dendrimer still localizes in the endosome, indicating that the endolysosomal vesicles are destabilized but they still retain their shape and some degree of integrity. This is of great importance to reduce the toxicity associated with the leakage of lysosomal enzymes. The similar performance for both dendrimers may be related to the proton sponge effect, which is characteristic of dendrimers rich in tertiary amines,^{3,10} which is the case for both the 2- and 4-arm derivatives. These cell-based studies are critical because they confirm the ability of our dendrimers to address two key issues in designing delivery platforms: cell internalization and endosomal escape.

Molecular Simulations. The biological results presented in the previous sections suggest a direct correlation between performance and the macromolecular structure with the number of amine end groups and architecture playing important roles. To investigate the details of these structural effects, molecular dynamics (MD) simulations were performed on the 2-armPEG-G4 and 4-armPEG-G4 dendrimers.

The structure of 2-armPEG-G4 was created and simulated according to the procedure described in the Computational Methods section of the SI. Figure 6a reports snapshots taken from the equilibrated phase of the MD simulation and shows that the PEG core of 2-armPEG-G4 dendrimer collapses into a globular shape, exposing the dendrons at both sides. Despite its relative hydrophilicity, the collapse of the polymer can be attributed to the tendency of the polymer to decrease the surface exposed to the surrounding aqueous solution. This is in good agreement with previous MD studies of dendrimers decorated with PEG chains.^{38,39} The swelling of the dendrons results from electrostatic repulsion between their charged amino end-groups groups with folding of the PEG core and stability of this collapsed structure being in good agreement with DLS measurements, which showed a diameter of 5 nm for the 2-armPEG-G4 and 9 nm for the 4-armPEG-G4 (SI).

Interestingly, MD of the 4-armPEG-G4 (Figure 6b) showed significantly different behavior with the PEG core of the 4-

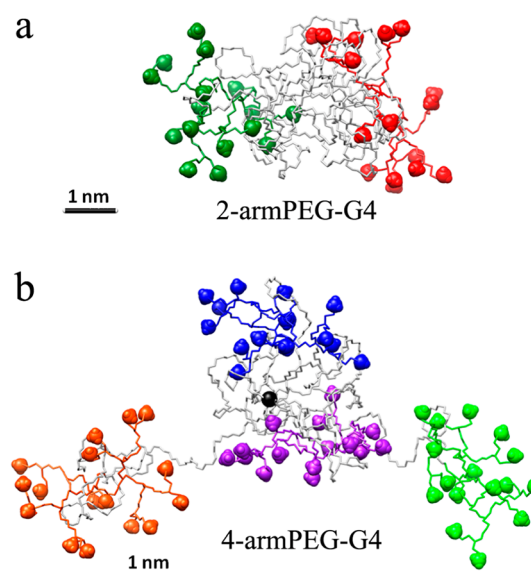


Figure 6. Molecular dynamics snapshot of the equilibrated structure for the 2-armPEG-G4 (a) and 4-armPEG-G4 (b) dendrimers. Simulations were carried out in water pH 7.4 containing 150 mM of NaCl.

armPEG-G4 dendrimer being less dense than the corresponding 2-arm derivative (Figure 6a). To understand the influence of architecture and core branching on the dynamic difference between 2-arm PEG and 4-arm PEG hybrid dendrimers, we calculated the average distances between each dendron and the center of the PEG core over the duration of the MD simulation. The plots reported in Figure 7, together with the snapshots taken from different time points during the simulation, illustrate the differences in dynamic behavior between the two dendrimer-PEG hybrids. From the simulations, it is evident that the equilibrated configuration of the 2-armPEG-G4 remains stable during the entire 200 ns of MD simulation (Figure 7a). In direct contrast, the 4-armPEG-G4 hybrid dendrimer assumes a much more dynamic structure with modeling, showing that the 4-arm PEG core can accommodate only two of the four dendrons stably (purple and blue D3 and D4 in Figure 7b), whereas the other two dendrons fluctuate away from the center. The “oscillatory” behavior of dendrons D1 and D2 (Figure 7b, red and green) is most likely due to a competition between the characteristic tendency of the PEG to fold and the electrostatic repulsion between the charged amine end groups. This leads to increased exposure of the dendrons to the surrounding aqueous environment and a reduced influence of the steric hindrance of the PEG core. It should be noted that this simulated phenomenon agrees well with the improved membrane-binding ability of the 4-arm-based hybrid dendrimer and with the transfection measurements, *vide infra*.

DNA Binding and Gene Transfection. The unique structural dynamics of the 4-armPEG-G4 coupled to the numerous cationic surface groups, cell-internalization ability, and endosomal destabilization suggests that these hybrid dendritic systems may be attractive candidates for binding of negatively charged DNA and subsequent delivery to the cytoplasm for gene-therapy applications.^{8,19} To evaluate the DNA binding ability of the 2-armPEG-G4 and 4-armPEG-G4 dendrimers, we performed an initial EB displacement assay. EB is known to emit red fluorescence upon intercalation into DNA. It has been reported that EB fluorescence is quenched by the

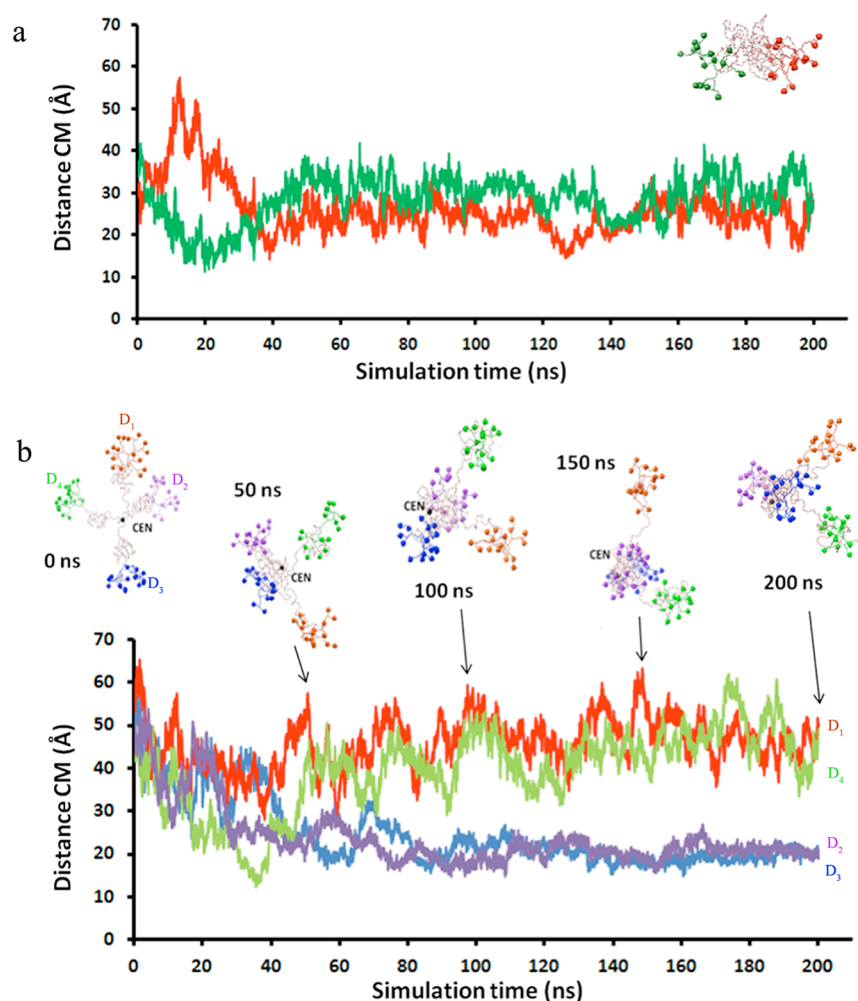


Figure 7. Plots of the distances between the centers of each dendron (D_n) and that of the PEG core for 2-armPEG-G4 (a) and 4-armPEG-G4 (b).

presence of a second molecule that can bind the nucleic acid with higher affinity, displacing the dye. DNA-EB complexes were therefore titrated with 2-armPEG-G4 and 4-armPEG-G4 (Figure 8a). The assay demonstrates that 4-armPEG-G4 has significantly higher affinity for DNA when compared with 2-arm derivative with a significantly faster drop in EB fluorescence with the 4-armPEG-G4's fluorescence signal plateauing at an N/P (the ratio between dendrimer amines versus DNA phosphates) of ca. 4, indicating a stable DNA-dendrimer complex, whereas the 2-armPEG-G4 requires a much higher N/P ratio (~ 15) to stabilize the dendriplex.

To analyze further the formation of 2- and 4-arm-based dendriplexes and study their ability to bind cell membranes, we mixed both types of dendrimers with Cy5-labeled DNA to form Cy5-labeled dendriplexes. The 2- and 4-arm dendriplexes were then incubated for 1 h with HeLa cells and single particles imaged using highly sensitive confocal spinning disk microscopy at the single cell level. Both 2- and 4-arm dendriplexes attached to the plasma membrane (Figure 8b); however, significantly lower fluorescence intensity was detected in the case of the 2-arm dendriplex particles (Figure 8c). This result supports the enhanced ability of 4-arm dendriplexes to bind DNA, as demonstrated in the EB intercalation assay. The amount of DNA delivered to HeLa cells after 22 h of incubation by the 2-arm and the 4-arm dendritic carriers was then quantified from the intensity of the fluorescence signal.

Significantly, the amount of DNA that was delivered by the 4-armPEG-G4 was nearly an order of magnitude greater than that for the 2-arm dendriplex (Figure 8c). This enhanced DNA delivery by the 4-arm dendriplex can be attributed to numerous property enhancements driven by changes due to the 4-arm architecture and higher number of amine end groups, which leads to improved DNA-binding efficacy.

To evaluate the actual transfection potential of the dendriplexes, we then used a plasmid encoding for green fluorescent protein bearing a nuclear localization signal (EGFP-Nuc) in combination with either the 2- or 4-arm dendrimer. The fluorescence arising from GFP expression allows the transfection efficiency to be quantified by widefield-fluorescence microscopy. Figure 8b,c shows the overlay of transmission light images for treated cells coupled to the green fluorescence signal for GFP expression, followed by quantification of the GFP fluorescence signals, respectively. It is particularly noteworthy that the 2-armPEG-G4 shows no apparent transfection, whereas a strong fluorescence signal from GFP expression following transfection with the 4-arm dendriplexes was observed. Because both dendrimers show endosome escaping abilities, the significant difference is probably related to the amount of DNA delivered to the cells. These results clearly show an enhanced ability for DNA delivery for the 4-armPEG-G4 platform compared with the corresponding 2-armPEG-G4 derivative. Because higher N/P

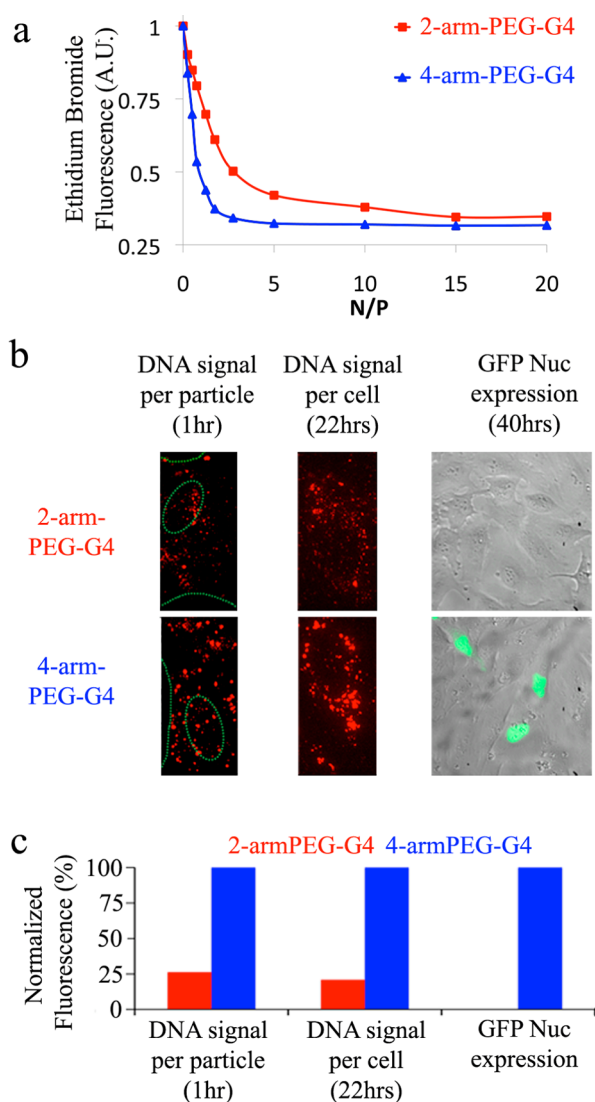


Figure 8. Dendrimer-mediated gene delivery: (a) EB intercalation assay and (b) confocal imaging (images widths are 30 μm for the left and center images and 205 μm for the image on the right) show dendriplex formation (left), cellular accumulation of dendriplexes (center), and the nuclear accumulation of the expressed GFP Nuc (green) overlaid on a transmission light image of treated cells (right). (c) Quantification of fluorescence signal (400 ng of DNA, $N/P = 4$, 240 μL).

ratio can influence the transfection efficiency, in particular, for the 2-arm dendrimer, the optimization of the transfection protocol in light of gene therapy is currently under further investigation.

CONCLUSIONS

Direct comparison between hybrid dendritic macromolecules based on 2- and 4-arm PEG cores has illustrated the influence of macromolecular architecture and core structure on their interactions with living cells. This leads to different biological properties which in turn can be related to a difference in solution structure with molecular dynamic studies showing that the 2-arm-PEG-G4 derivatives fold into a particle-like structure, with a compact, collapsed PEG core, whereas the 4-arm-PEG-G4 possesses a much less dense PEG core, resulting in a dynamic and oscillatory behavior in solution. Whereas both

dendrimers showed low toxicity and induced endosomal escape, the dynamic nature of the 4-arm hybrid translates to enhanced biological performance, resulting in improved cell affinity and internalization. Significantly, the 4-arm-PEG based dendrimer also showed dramatically improved DNA binding and gene transfection capabilities in cell culture, demonstrating the potential of these synthetically accessible dendrimers as intracellular delivery platforms for a wide variety of applications.

ASSOCIATED CONTENT

Supporting Information

MALDI-TOF MS, ^1H NMR spectra, dynamic light scattering results, and computational methods. This material is available free of charge via the Internet at <http://pubs.acs.org>.

AUTHOR INFORMATION

Corresponding Author

*E-mail: hawker@mrl.ucsb.edu (C.J.H.), amirroey@tau.ac.il (R.J.A.).

Notes

The authors declare no competing financial interest.

ACKNOWLEDGMENTS

This material is based on work supported by the National Institutes of Health as a Program of Excellence in Nanotechnology (HHSN268201000046C) (R.J.A., C.J.H.). This work was partially supported by the Institute for Collaborative Biotechnologies through grant numbers W911NF-07-1-0279 and W911NF-09-D-0001 from the U.S. Army Research Office (E.A., K.L.K., C.J.H.), MRSEC Program of the National Science Foundation through the MRL Central Facilities (L.A., K.L.K., C.J.H.) the Nanoinitiative Munich (NIM), the Elitenetzwerk Bayern, the SPP1313 and by fellowship support from Samsung (T.K.).

REFERENCES

- (1) Menjoge, A. R.; Kannan, R. M.; Tomalia, D. A. *Drug Discovery Today* **2010**, *15*, 171–185.
- (2) Bonduelle, C. V.; Gillies, E. R. *Pharmaceuticals* **2010**, *3*, 636–666.
- (3) Calderón, M.; Quadir, M. A.; Sharma, S. K.; Haag, R. *Adv. Mater.* **2010**, *22*, 190–218.
- (4) Cheng, Y.; Zhao, L.; Li, Y.; Xu, T. *Chem. Soc. Rev.* **2011**, *40*, 2673–2703.
- (5) Kaminskas, L. M.; Boyd, B. J.; Porter, C. J. H. *Nanomedicine* **2011**, *6*, 1063–1084.
- (6) Soliman, G. M.; Sharma, A.; Maysinger, D.; Kakkar, A. *Chem. Commun.* **2011**, *47*, 9572–9587.
- (7) El Kazzouli, S.; Mignani, S.; Bousmina, M.; Majoral, J. P. *New J. Chem.* **2012**, *36*, 227–240.
- (8) Bonner, D. K.; Leung, C.; Chen-Liang, J.; Chingozha, L.; Langer, R.; Hammond, P. T. *Bioconjugate Chem.* **2011**, *22*, 1519–1525.
- (9) Mintzer, M. A.; Simanek, E. E. *Chem. Rev.* **2009**, *109*, 259–302.
- (10) Turrin, C. O.; Caminade, A. M. In *Dendrimers: Towards Catalytic, Material and Biomedical Uses*; Caminade, A. M., Turrin, C. O., Laurent, R., Ouali, A., Delavaux-Nicot, B., Eds.; John Wiley & Sons, Ltd.: Chichester, U.K., 2011; pp 413–435.
- (11) Mumper, R. J.; Bell, M. A.; Worthen, D. R.; Cone, R. A.; Lewis, G. R.; Paull, J. R. A.; Moench, T. R. *Drug Dev. Ind. Pharm.* **2009**, *35*, 515–524.
- (12) Heegaard, P. M. H.; Boas, U.; Sorensen, N. S. *Bioconjugate Chem.* **2010**, *21*, 405–418.
- (13) Skwarczynski, M.; Zaman, M.; Urbani, C. N.; Lin, I.; Jia, Z.; Batzloff, M. R.; Good, M. F.; Monteiro, M. J.; Toth, I. *Angew. Chem., Int. Ed.* **2010**, *49*, 5742–5745.

- (14) Antoni, P.; Robb, M. J.; Campos, L.; Montanez, M.; Hult, A.; Malmstorm, E.; Malkoch, M.; Hawker, C. J. *Macromolecules* **2010**, *43*, 6625–6631.
- (15) Duncan, R.; Izzo, L. *Adv. Drug Delivery Rev.* **2005**, *57*, 2215–2237.
- (16) Fernandez-Megia, E.; Correa, J.; Riguera, R. *Biomacromolecules* **2006**, *7*, 3104–3111.
- (17) Clementi, C.; Miller, K.; Mero, A.; Satchi-Fainaro, R.; Pasut, G. *Mol. Pharmaceutics* **2011**, *8*, 1063–1072.
- (18) Sousa-Herves, A.; Riguera, R.; Fernandez-Megia, E. *New J. Chem.* **2011**, *36*, 205–210.
- (19) Kim, T.; Seo, H. J.; Choi, J. S.; Jang, H. S.; Baek, J.; Kim, K.; Park, J. S. *Biomacromolecules* **2004**, *5*, 2487–2492.
- (20) Amir, R. J.; Albertazzi, L.; Willis, J.; Khan, A.; Kang, T.; Hawker, C. J. *Angew. Chem., Int. Ed.* **2011**, *50*, 3425–3429.
- (21) Lowe, A. B.; Hoyle, C. E.; Bowman, C. N. *J. Mater. Chem.* **2010**, *20*, 4745–4750.
- (22) Silvers, A. L.; Chang, C. C.; Emrick, T. *J. Polym. Sci., Part A: Polym. Chem.* **2012**, *50*, 3517–3529.
- (23) Chen, G.; Kumar, J.; Gregory, A.; Stenzel, M. H. *Chem. Commun.* **2009**, *41*, 6291–6293.
- (24) Kolb, H. C.; Sharpless, K. B. *Drug Discovery Today* **2003**, *8*, 1128–1137.
- (25) Wang, D. K.; Hill, D. J. T.; Rasoul, F. A.; Whittaker, A. K. *J. Polym. Sci., Part A: Polym. Chem.* **2012**, *50*, 1143–1157.
- (26) Wu, Z.; Zeng, X.; Zhang, Y.; Feliu, N.; Lundberg, P.; Fadeel, B.; Malkoch, M.; Nyström, A. M. *J. Polym. Sci., Part A: Polym. Chem.* **2012**, *50*, 217–226.
- (27) Albertazzi, L.; Serresi, M.; Albanese, A.; Beltram, F. *Mol. Pharmaceutics* **2010**, *7*, 680–688.
- (28) Albertazzi, L.; Storti, B.; Marchetti, L.; Beltram, F. *J. Am. Chem. Soc.* **2010**, *132*, 18158–18167.
- (29) Reichert, S.; Welker, P.; Calderón, M.; Khandare, J.; Mangoldt, D.; Licha, K.; Kainthan, R. K.; Brooks, D. E.; Haag, R. *Small* **2011**, *7*, 820–829.
- (30) Iliashevsky, O.; Amir, L.; Glaser, R.; Marks, R. S.; Lemcoff, N. G. *J. Mater. Chem.* **2009**, *19*, 6616–6622.
- (31) Kelly, C. V.; Liroff, M. G.; Triplett, L. D.; Leroueil, P. R.; Mullen, D. G.; Wallace, J. M.; Meshinchi, S.; Baker, J. R.; Orr, B. G.; Banaszak Holl, M. M. *ACS Nano* **2009**, *3*, 1886–1896.
- (32) Jones, S. P.; Gabrielsen, N. P.; Wong, C. H.; Chow, H. F.; Pack, D.; Posocco, P.; Fermeglia, M.; Prich, S.; Smith, D. K. *Mol. Pharmaceutics* **2011**, *8*, 416–429.
- (33) Bastings, M. M. C.; Helms, B. A.; van Baal, I.; Hackeng, T. M.; Merkx, M.; Meijer, E. *J. Am. Chem. Soc.* **2011**, *133*, 6636–6641.
- (34) Fox, M. E.; Guillaudeu, S.; Fréchet, J. M. J.; Jerger, K.; Macaraeg, N.; Szoka, F. C. *Mol. Pharmaceutics* **2009**, *6*, 1562–1572.
- (35) Kurtoglu, Y. E.; Navath, R. S.; Wang, B.; Kannan, S.; Romero, R.; Kannan, R. M. *Biomaterials* **2009**, *30*, 2112–2121.
- (36) Lo Conte, M.; Robb, M. J.; Hed, Y.; Marra, A.; Malkoch, M.; Hawker, C. J.; Dondoni, A. *J. Polym. Sci., Part A: Polym. Chem.* **2011**, *49*, 4468–4475.
- (37) Albertazzi, L.; Fernandez-Villamarin, M.; Giuera, R.; Fernandez-Megia, R. *Bioconjugate Chem.* **2012**, *23*, 1059–1068.
- (38) Pavan, G. M.; Mintzer, M. A.; Simanek, E. E.; Merkel, O. M.; Kissel, T.; Danani, A. *Biomacromolecules* **2010**, *11*, 721–730.
- (39) Albertazzi, L.; Brondi, M.; Pavan, G. M.; Sulis Sato, S.; Signore, G.; Storti, B.; Ratto, G. M.; Beltram, F. *PLoS ONE* **2011**, *6*, e28450.